Binuclear and Polymeric Manganese(II) Salicylate Complexes: Synthesis, Crystal Structure and Catalytic Activity of $[Mn_2(Hsal)_4(H_2O)_4]$ and $[\{Mn_2(sal)_2(Hsal)(H_2O)(H_3O)(py)_4\cdot 2py\}_n]$ (H_2sal = salicylic acid, py = pyridine)†

Michael Devereux,*[a] Malachy McCann,*[b] Michael T. Casey,[b] Martin Curran,[a] George Ferguson,*[c] Christine Cardin,*[d] Moira Convery[e] and Valerie Quillet[f]

[a] *Dublin Institute of Technology, Cathal Brugha Street, Dublin, Ireland*
[b] *Chemistry Department, St. Patrick's College, Maynooth, Co. Kildare, Ireland*
[c] *Department of Chemistry and Biochemistry, University of Guelph, Ontario N1G 2W1, Canada*
[d] *Department of Chemistry, The University, Whiteknights, Reading RG6 2AD, UK*
[e] *Department of Biochemistry and Molecular Biology, University of Leeds, Leeds LS2 9JT, UK*
[f] *Chemistry Department, Trinity College, Dublin, Ireland*

The two air-stable manganese(II) salicylate complexes $[Mn_2(Hsal)_4(H_2O)_4]$ **1** and polymeric $[\{Mn_2(sal)_2(Hsal)(H_2O)(H_3O)(py)_4\cdot 2py\}_n]$ **2** (H_2sal = salicylic acid and py = pyridine) have been synthesised easily, and their crystal structures determined. Both contain unsymmetrically bridging salicylate ligands. In the presence of added pyridine **1** and **2** vigorously catalyse the disproportionation of H_2O_2.

The current intense interest in carboxylate bridged bi- and poly-nuclear manganese complexes has been fuelled by the identification of an increasing number of Mn-containing enzymes, and much effort has been expended on the study of the nature of the bridging mode of the carboxylate groups in these systems.[1,2] It has been suggested[3] that salicylic acid (2-hydroxybenzoic acid) (H_2sal) is a convenient ligand substitute for the 'biologically relevant' tyrosine phenoxide and aspartic/glutamic carboxylate functions. With this in mind Christou and co-workers[3,4] prepared and structurally characterised the dimanganese(III,III) dianionic complex[3] $[Mn_2(sal)_4(py)_2]^{2-}$ (py = pyridine) and the mixed-valence nonanuclear oxide-bridged complex $[Mn_9O_4(O_2CPh)_8(sal)_4(Hsal)_2(py)_4]$.[4] The study of complexation of metals by salicylate ions is important also because the bonding in such complexes can serve as useful models for the interaction of these metals with humic materials in the natural environment.[5] Here we report the facile syntheses, crystal structures and properties of two manganese(II) salicylate complexes, $[Mn_2(Hsal)_4(H_2O)_4]$ **1** and polymeric $[\{Mn_2(sal)_2(Hsal)(H_2O)(H_3O)(py)_4\cdot 2py\}_n]$ **2**, which both contain unsymmetrically bridging salicylate ligands.

Results and Discussion

The preparations of complexes **1** and **2** are summarised in Scheme 1. The crystal structure of complex **1** is shown in Fig. 1.

$$MnCl_2\cdot 4H_2O + Na(Hsal) \xrightarrow{H_2O} [Mn_2(Hsal)_4(H_2O)_4]\ \mathbf{1}$$

$$\xrightarrow{py} [\{Mn_2(sal)_2(Hsal)(H_2O)(H_3O)(py)_4\cdot 2py\}_n]\ \mathbf{2}$$

Scheme 1

† *Supplementary data available:* see Instructions for Authors, *J. Chem. Soc., Dalton Trans.*, 1995, Issue 1, pp. xxv–xxx.

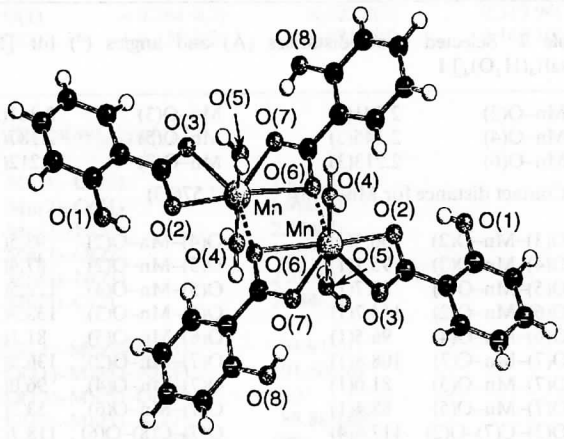

Fig. 1 Structure of $[Mn_2(Hsal)_4(H_2O)_4]$ **1**

Fractional atomic coordinates are listed in Table 1, and selected bond distances and angles in Table 2. The complex is comprised of two associated and symmetry related pseudo seven-co-ordinate Mn^{II} centres (Mn–Mn distance 3.719 Å). Each Mn is asymmetrically chelated by two $Hsal^-$ ($HOC_6H_4CO_2^-$) ligands, and perpendicular to the central plane there are two co-ordinated water molecules. Association of the two metals occurs *via* the carboxylate oxygen atoms [O(6)] from a second pair of chelating $Hsal^-$ ligands, effectively creating two asymmetric bridges between the Mn atoms [Mn–O(6) 2.213(3) and 2.576(3) Å]. A similar type of monodentate carboxylate oxygen bridge was reported by Kitajima and co-workers[1] for the benzoate complex $[\{HB(C_3N_2HPr^i_2\text{-}3,5)_3\}Mn(\mu\text{-}O_2CPh)Mn(C_3N_2H_2Pr^i_2\text{-}3,5)]$ [$HB(C_3N_2HPr^i_2\text{-}3,5)_3$ = hydrotris(3,5-diisopropylpyrazol-1-yl)borate, $C_3N_2H_2Pr^i_2$-3,5 = 3,5-diisopropylpyrazole]. Lippard and co-workers[6] have postulated that the carboxylate monodentate bridging mode [Fig. 2(*a*)] is an important intermediate between the other, more common

Table 1 Fractional atomic coordinates for $[Mn_2(Hsal)_4(H_2O)_4]$ **1**

Atom	*x*	*y*	*z*
Mn	0.007 26(7)	0.397 16(4)	0.087 44(4)
C(1)	0.179 7(6)	0.141 0(4)	0.333 3(3)
C(2)	0.252 3(8)	0.096 2(5)	0.410 4(4)
C(3)	0.313 7(8)	0.163 5(6)	0.475 8(4)
C(4)	0.304 7(7)	0.273 4(5)	0.468 0(3)
C(5)	0.230 8(5)	0.320 4(4)	0.391 2(3)
C(6)	0.167 3(5)	0.252 9(3)	0.322 3(2)
C(7)	0.093 3(5)	0.298 9(3)	0.239 5(2)
C(8)	−0.001 4(4)	0.329 7(3)	−0.081 6(2)
C(9)	0.033 0(5)	0.275 2(3)	−0.161 5(2)
C(10)	0.068 3(6)	0.335 8(4)	−0.232 9(3)
C(11)	0.105 9(6)	0.286 2(4)	−0.307 6(3)
C(12)	0.109 6(6)	0.173 7(4)	−0.311 8(3)
C(13)	0.077 9(6)	0.112 0(4)	−0.242 4(3)
C(14)	0.037 9(5)	0.162 0(3)	−0.167 6(2)
O(1)	0.222 1(6)	0.429 6(3)	0.386 6(3)
O(2)	0.080 0(4)	0.401 2(2)	0.230 5(2)
O(3)	0.044 0(4)	0.240 1(2)	0.174 3(2)
O(4)	−0.269 6(4)	0.413 3(3)	0.097 0(2)
O(5)	0.289 6(4)	0.403 7(3)	0.074 9(2)
O(6)	−0.010 8(4)	0.430 6(2)	−0.076 1(2)
O(7)	−0.019 9(4)	0.272 5(2)	−0.015 1(2)
O(8)	0.005 9(4)	0.097 4(2)	−0.099 6(2)
H(1)	0.124 4(68)	0.100 5(40)	0.283 8(33)
H(2)	0.218 7(66)	0.021 4(44)	0.407 6(31)
H(3)	0.359 5(80)	0.127 1(50)	0.525 7(41)
H(4)	0.328 9(70)	0.323 8(45)	0.513 5(33)
H(5)	0.182 4(89)	0.449 3(55)	0.345 4(41)
H(6)	0.189 8(66)	0.130 4(43)	0.111 5(31)
H(7)	0.184 7(56)	0.021 7(40)	0.110 6(27)
H(8)	0.849 9(67)	0.038 3(43)	0.078 7(32)
H(9)	0.862 5(57)	0.127 0(36)	0.107 0(26)

Table 2 Selected bond distances (Å) and angles (°) for $[Mn_2(Hsal)_4(H_2O)_4]$ **1**

Mn–O(2)	2.241(3)	Mn–O(3)	2.361(3)
Mn–O(4)	2.145(3)	Mn–O(5)	2.187(3)
Mn–O(6)	2.213(3)	Mn–O(7)	2.212(3)
Contact distance for Mn–O(6)		2.576(3)	
O(3)–Mn–O(2)	56.3(1)	O(4)–Mn–O(2)	93.5(1)
O(4)–Mn–O(3)	95.1(1)	O(5)–Mn–O(2)	87.4(1)
O(5)–Mn–O(3)	91.7(1)	O(5)–Mn–O(4)	172.5(1)
O(6)–Mn–O(2)	164.7(1)	O(6)–Mn–O(3)	133.7(1)
O(6)–Mn–O(4)	96.5(1)	O(6)–Mn–O(5)	81.1(1)
O(7)–Mn–C(7)	108.8(1)	O(7)–Mn–O(2)	136.9(1)
O(7)–Mn–O(3)	81.0(1)	O(7)–Mn–O(4)	96.0(1)
O(7)–Mn–O(5)	88.4(1)	O(7)–Mn–O(6)	53.3(1)
O(3)–C(7)–O(2)	117.6(4)	O(7)–C(8)–O(6)	118.7(3)

attachment modes. In Kitajima and co-workers'[1] complex the three Mn–O(benzoate) bond distances are almost the same [Fig. 2(*b*)], whereas in complex **1** the salicylates are in a unique bridging mode in that the monoatomic oxygen bridge is highly asymmetric [Fig. 2(*c*)]. The stability of complex **1** in the solid state is further enhanced by intramolecular hydrogen bonding between the hydroxyl groups of the $Hsal^-$ function and one carboxylate oxygen [O(7)] of the same ligand.

Although a few dimanganese(II,II) complexes containing symmetrical *syn–syn* carboxylate bridges (μ-O_2CR) have been structurally characterised[7] it seems that $[\{HB(C_3N_2HPr^i{}_2\text{-}3,5)_3\}Mn(\mu\text{-}O_2CPh)_3Mn(C_3N_2H_2Pr^i{}_2\text{-}3,5)_2]$[1] and $[Mn_2(Hsal)_4(H_2O)_4]$ **1** are the only dinuclear Mn^{II} species known where one of the bridging carboxylate oxygen atoms is bonded to the two metal centres. These structures may have important implications in Lippard's 'carboxylate shift' phenomenon which relates to the structure, function and kinetics of carboxylate-containing metalloproteins.[6]

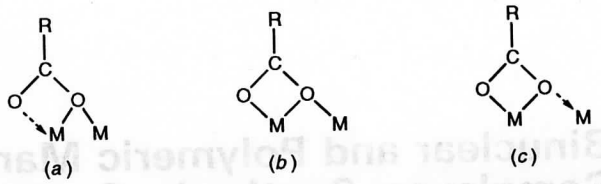

Fig. 2 Carboxylate bridging modes in complexes **1** and related species: (*a*) ref. 7, (*b*) ref. 1, (*c*) this work

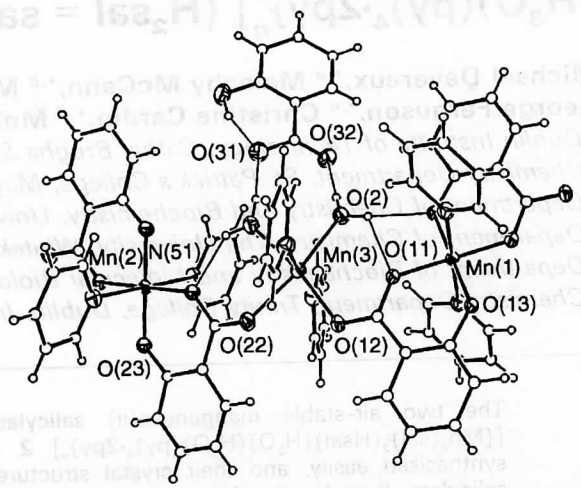

Fig. 3 Structure of $[\{Mn_2(sal)_2(Hsal)(H_2O)(H_3O)(py)_4\cdot 2py\}_n]$ **2** (pyridine molecules of crystallisation not shown)

The crystal structure of $[\{Mn_2(sal)_2(Hsal)(H_2O)(H_3O)(py)_4\cdot 2py\}_n]$ **2** is shown in Fig. 3. Fractional atomic coordinates are listed in Table 3, and selected bond distances and angles in Table 4. The structure comprises three independent Mn^{II} atoms [Mn(1), Mn(2) and Mn(3)] in a polymeric system of the type shown below.

. . Mn(1) . . . Mn(3) . . . Mn(2) . . . Mn(3) . . . Mn(1) . . .
Mn(3) . . . Mn(2) . . . Mn(3) . . . Mn(1) . .

Atom Mn(1) [Fig. 4(*a*)] lies on an inversion centre and is bonded to a carboxyl oxygen [O(11)] and a hydroxyl oxygen [O(13)] (both from a sal^{2-} ligand), and also to a pyridine nitrogen; Mn(2) [Fig. 4(*b*)] lies on another inversion centre and it has an N_2O_4 octahedral co-ordination geometry identical to that of Mn(1); Mn(3) [Fig. 4(*c*)] is in a general position, and is bonded to the second carboxylate oxygen [O(12)] from the sal^{2-} ligand which is co-ordinated to Mn(1), and also to the second carboxylate oxygen [O(22)] from the sal^{2-} ligand which is co-ordinated to Mn(2). The co-ordination mode of the carboxylate moieties of both of these bridging sal^{2-} ligands is *syn–anti* bidentate, with O(12) and O(22) ending up in a *cis* position about Mn(3). The oxygen [O(2)] of a water molecule and the oxygen [O(1)] of a cisoid oxonium ion (H_3O^+) are also co-ordinated to Mn(3), and the N_2O_4 octahedral co-ordination about the metal is completed by two axial pyridine ligands. Furthermore, a $Hsal^-$ ion is hydrogen bonded *via* its carboxylate oxygens [O(31) and O(32)] in a *syn–syn* bidentate bridging mode to the water molecule and to the oxonium ion which are co-ordinated to Mn(3). Additional inter-ligand hydrogen-bonding interactions are shown in Fig. 3. It is notable that whereas the bond angles between cisoid ligands about Mn(1) and Mn(2) are close to 90° those around Mn(3) deviate by as much as *ca.* 18° from this value, and confirm the highly distorted octahedral geometry about this metal centre. In addition, the Mn(3)–O(carboxylate) bond distances are significantly greater than those about Mn(1) and Mn(2). Finally, two pyridine molecules of solvation were also

Table 3 Fractional atomic coordinates for $[\{Mn_2(sal)_2(Hsal)(H_2O)(H_3O)(py)_4\cdot 2py\}_n]$ **2**

Atom	*x*	*y*	*z*
Mn(1)	0	0	0
Mn(2)	$-\frac{1}{2}$	0	$\frac{1}{2}$
Mn(3)	−0.202 77(5)	0.011 34(4)	0.257 42(4)
C(11)	−0.042 9(3)	−0.187 1(2)	0.122 2(2)
C(12)	0.030 5(3)	−0.179 6(2)	0.053 9(2)
C(13)	0.070 2(3)	−0.259 3(3)	0.034 7(2)
C(14)	0.036 4(4)	−0.345 0(3)	0.080 2(3)
C(15)	−0.037 2(4)	−0.353 1(3)	0.146 8(3)
C(16)	−0.076 1(3)	−0.275 3(3)	0.166 9(2)
C(17)	−0.085 4(3)	−0.105 4(2)	0.151 1(2)
O(11)	−0.057 7(2)	−0.022 84(17)	0.112 04(14)
O(12)	−0.145 5(2)	−0.113 86(18)	0.214 73(15)
O(13)	0.066 5(2)	−0.100 08(17)	0.005 65(14)
C(21)	−0.437 9(3)	−0.199 4(3)	0.428 3(2)
C(22)	−0.538 6(3)	−0.215 5(3)	0.476 9(2)
C(23)	−0.603 0(3)	−0.315 8(3)	0.496 6(3)
C(24)	−0.573 7(4)	−0.397 2(3)	0.468 7(3)
C(25)	−0.478 9(4)	−0.382 9(3)	0.419 2(3)
C(26)	−0.412 8(4)	−0.285 6(3)	0.400 0(2)
C(27)	−0.359 0(3)	−0.096 8(3)	0.406 6(2)
O(21)	−0.375 0(2)	−0.015 58(17)	0.436 28(14)
O(22)	−0.276 5(2)	−0.089 31(19)	0.360 20(16)
O(23)	−0.573 31(19)	−0.141 51(17)	0.505 62(14)
C(31)	−0.314 2(3)	0.395 9(3)	0.160 3(2)
C(32)	−0.347 9(3)	0.457 0(3)	0.218 6(2)
C(33)	−0.375 7(4)	0.538 0(3)	0.190 9(3)
C(34)	−0.369 2(4)	0.556 8(3)	0.106 2(3)
C(35)	−0.335 6(4)	0.497 3(3)	0.048 1(3)
C(36)	−0.307 0(3)	0.417 9(3)	0.075 1(3)
C(37)	−0.288 4(3)	0.305 5(3)	0.186 9(3)
O(31)	−0.295 6(3)	0.290 0(2)	0.266 6(2)
O(32)	−0.263 2(3)	0.250 9(2)	0.131 80(19)
O(33)	−0.358 8(3)	0.439 6(2)	0.302 33(19)
N(41)	0.174 0(3)	0.127 8(2)	0.057 31(19)
C(42)	0.276 7(4)	0.133 5(4)	0.028 6(3)
C(43)	0.380 2(4)	0.214 3(5)	0.053 2(4)
C(44)	0.378 2(5)	0.294 5(4)	0.108 4(4)
C(45)	0.274 0(5)	0.287 5(4)	0.140 0(4)
C(46)	0.174 9(4)	0.203 9(3)	0.112 3(3)
N(51)	−0.607 9(3)	−0.010 6(2)	0.370 00(19)
C(52)	−0.588 2(4)	0.070 7(3)	0.325 8(3)
C(53)	−0.657 8(5)	0.070 4(4)	0.254 2(3)
C(54)	−0.752 0(5)	−0.018 4(5)	0.226 6(3)
C(55)	−0.771 6(4)	−0.103 0(4)	0.269 1(3)
C(56)	−0.697 7(4)	−0.096 7(4)	0.340 5(3)
N(61)	−0.022 9(3)	0.093 1(2)	0.326 5(2)
C(62)	0.028 3(5)	0.044 2(4)	0.373 6(3)
C(63)	0.138 0(6)	0.090 6(5)	0.414 9(4)
C(64)	0.198 5(5)	0.193 1(6)	0.408 0(4)
C(65)	0.146 9(5)	0.246 0(4)	0.361 4(4)
C(66)	0.037 3(4)	0.192 4(4)	0.322 4(3)
N(71)	−0.380 4(3)	−0.078 7(3)	0.183 1(2)
C(72)	−0.442 9(4)	−0.032 7(4)	0.144 0(3)
C(73)	−0.553 6(6)	−0.085 6(6)	0.104 9(4)
C(74)	−0.602 0(5)	−0.190 0(7)	0.105 9(5)
C(75)	−0.540 2(5)	−0.239 7(4)	0.145 3(4)
C(76)	−0.429 7(4)	−0.181 5(4)	0.182 8(3)
N(81)	0.234 0(4)	0.532 5(3)	0.177 7(3)
C(82)	0.133 6(5)	0.459 7(4)	0.146 8(3)
C(83)	0.037 0(5)	0.419 7(4)	0.191 6(5)
C(84)	0.042 3(6)	0.455 6(5)	0.275 0(5)
C(85)	0.144 2(7)	0.531 1(6)	0.310 0(4)
C(86)	0.237 0(6)	0.566 3(5)	0.259 3(5)
N(91)	0.081 5(8)	0.735 5(11)	0.496 3(7)
C(92)	0.015 9(12)	0.631 6(10)	0.497 6(7)
C(93)	−0.080 7(9)	0.593 1(5)	0.451 0(6)
C(94)	−0.121 2(6)	0.648 6(6)	0.404 5(4)
C(95)	−0.062 2(9)	0.748 8(7)	0.405 9(4)
C(96)	0.035 9(9)	0.793 5(6)	0.450 1(7)
O(1)	−0.264 4(2)	0.125 2(2)	0.319 94(16)
O(2)	−0.159 8(2)	0.121 4(2)	0.160 10(16)

Table 4 Selected bond distances (Å) and angles (°) for $[\{Mn_2(sal)_2(Hsal)(H_2O)(H_3O)(py)_4\cdot 2py\}_n]$ **2**

Mn(1)–O(11)	1.914(2)	Mn(1)–O(13)	1.879(2)
Mn(1)–N(41)	2.310(2)	Mn(2)–O(21)	1.930(2)
Mn(2)–O(23)	1.862(2)	Mn(2)–N(51)	2.344(3)
Mn(3)–O(12)	2.198(2)	Mn(3)–O(22)	2.207(2)
Mn(3)–N(61)	2.257(3)	Mn(3)–N(71)	2.287(3)
Mn(3)–O(1)	2.197(3)	Mn(3)–O(2)	2.184(2)
O(11)–Mn(1)–O(11^{i})	180	O(11)–Mn(1)–O(13)	91.91(9)
O(11)–Mn(1)–O(13^{i})	88.09(9)	O(11)–Mn(1)–N(41)	91.50(10)
O(11)–Mn(1)–N(41^{i})	88.50(10)	O(13)–Mn(1)–O(13^{i})	180
O(13)–Mn(1)–N(41)	91.12(10)	O(13)–Mn(1)–N(41^{i})	88.88(10)
N(41)–Mn(1)–N(41^{i})	180	O(21)–Mn(2)–O(21^{ii})	180
O(21)–Mn(2)–O(23)	92.25(9)	O(21)–Mn(2)–O(23^{ii})	87.75(9)
O(21)–Mn(2)–N(51)	89.75(10)	O(21)–Mn(2)–N(51^{ii})	90.25(10)
O(23)–Mn(2)–O(23^{ii})	180	O(23)–Mn(2)–N(51)	91.08(11)
O(23)–Mn(2)–N(51^{ii})	88.92(11)	N(51)–Mn(2)–N(51^{ii})	180
O(12)–Mn(3)–O(22)	82.50(9)	O(12)–Mn(3)–N(71)	88.52(11)
O(12)–Mn(3)–O(1)	170.74(9)	O(12)–Mn(3)–O(2)	107.81(9)
O(22)–Mn(3)–N(61)	95.26(11)	O(22)–Mn(3)–N(71)	85.00(11)
O(22)–Mn(3)–O(1)	88.61(9)	O(22)–Mn(3)–O(2)	168.15(9)
O(1)–Mn(3)–O(2)	81.31(9)	N(61)–Mn(3)–N(71)	176.32(12)
N(61)–Mn(3)–O(2)	91.05(11)	N(71)–Mn(3)–O(1)	93.28(12)
N(71)–Mn(3)–O(2)	89.36(11)	N(61)–Mn(3)–O(1)	90.39(11)

Superscripts i and ii refer to equivalent positions $-x, -y, -z$ and $-1-x, -y, 1-z$, respectively.

located but have been omitted from Fig. 3 for clarity. The empirical formula of **2** is thus $Mn_2(sal)_2(Hsal)(H_2O)(H_3O)(py)_4\cdot 2py$.

The structures of both **1** and **2** are significantly different to Christou and co-workers'[3,4] dimanganese(III,III) complex dianion[3] $[Mn_2(sal)_4(py)_2]^{2-}$ and mixed-valence nonanuclear oxide-bridged complex $[Mn_9O_4(O_2CPh)_8(sal)_4(Hsal)_2(py)_4]$.[4] The dianion $[Mn_2(sal)_4(py)_2]^{2-}$ consists of two octahedral Mn^{III} atoms bridged by two μ-phenoxo oxygen atoms from a pair of sal^{2-} groups. One carboxylate oxygen from each of these

bridging sal^{2-} groups is also bound to the metal. Each Mn^{III} additionally contains a py and another sal^{2-}, the latter group chelating *via* the phenoxo oxygen and one carboxylate oxygen. The complex $[Mn_9O_4(O_2CPh)_8(sal)_4(Hsal)_2(py)_4]$ consists of two butterfly-like $Mn_4(\mu_3\text{-}O)_2$ units, containing octahedral Mn^{III} ions, linked together by a bridging $Mn(sal)_4$ central unit. The latter contains an eight-co-ordinate Mn^{II} ion. The sal^{2-} groups linking the Mn^{II} and Mn_4O_2 units have a μ_3–η^3-bridging mode; peripheral ligation to the complete molecule is provided by eight μ-O_2CPh, four terminal py, and two μ-$Hsal^-$ groups, employing only their carboxylate functions with the phenoxide oxygen atoms protonated and unco-ordinated.

The magnetic moment of a powdered sample of complex **1** (μ = 5.78 μ_B per Mn at 300 K or 5.70 μ_B at 80 K) showed that there was no significant exchange interaction between the metal centres. Complex **2** had a room temperature magnetic moment of μ = 5.73 μ_B per Mn. These magnetic moments for **1** and **2** are close to those expected for normal Mn^{II} complexes.[8]

Complexes **1** and **2** both appear to be air-stable in the solid state and in solution, and their relative insensitivity towards oxidation was further substantiated by electrochemical studies. The cyclic voltammogram of an aqueous solution of complex **1** showed no redox behaviour between the switching potentials of −1.25 and +1.30 V (*versus* Ag–AgCl). Between +0.20 V and +1.70 V the voltammogram of an ethanolic solution of complex **2** showed a metal-centred irreversible oxidation wave at the highly anodic potential of E_c = +1.45 V.

We have recently described the synthesis and structure of the dimanganese(II,II) complex double salt $[Mn_2(\mu\text{-oda})(phen)_4(H_2O)_2][Mn_2(\mu\text{-oda})(phen)_4(oda)_2]\cdot 4H_2O$ (H_2oda = octanedioic acid and phen = 1,10-phenanthroline), and demonstrated the ability of the complex to catalyse the disproportionation of H_2O_2 [equation (1)].[9]

$$2H_2O_2 \longrightarrow 2H_2O + O_2 \qquad (1)$$

The aptitude of complexes **1** and **2** as catalysts for this disproportionation reaction was also investigated. Whereas **1** alone did not decompose H_2O_2 it was found that the presence of added pyridine was an extremely active combination for disproportionation. During the first 60 s of the latter reaction each molecule of **1** on average disproportionated 1552 molecules of H_2O_2. The reaction of **2** alone with H_2O_2 was also very sluggish, and typically only about 100 molecules of H_2O_2 were decomposed per molecule of **2** over the first 150 s of the reaction. However, when **2** was dissolved in pyridine the catalytic activity was greatly enhanced, and during the first 150 s each molecule of **2** disproportionated 2924 molecules of H_2O_2.

The above results show that addition of the base pyridine causes a significant increase in the catalytic activity of the Mn^{II} complexes **1** and **2** towards H_2O_2. This observation may help significantly in our understanding of the role of nitrogen-containing heterocyclic bases which are known to be located in the vicinity of the active sites of manganocatalases.[10] In their work with Mn^{III} porphyrin dimers Naruta and Maruyama[11] reported that in the absence of the base 1-methylimidazole none of their complexes decomposed H_2O_2. However, on adding the imidazole some (but not all) of the complexes showed high oxygen-evolving activity. Earlier, it had been reported that the role of imidazole in H_2O_2–Mn porphyrin systems was to accelerate the O–O bond homolysis and also to stabilise a Mn^{IV}=O intermediate complex.[12] Larson and Pecoraro[13] showed that the monomeric Mn^{III} complex $[Mn(salpn)(MeOH)_2]ClO_4$ [H_2salpn = propane-1,3-diylbis(salicylideneimine)] is unreactive towards H_2O_2 unless base (NaOH or NaOMe) is added. In this reaction the oxidised Mn^{IV} dimer $[Mn_2(salpn)_2(O)_2]$ is formed, and it is thought that the role of the added base is to deprotonate the H_2O_2 prior to its reaction with the Mn^{III} monomer.

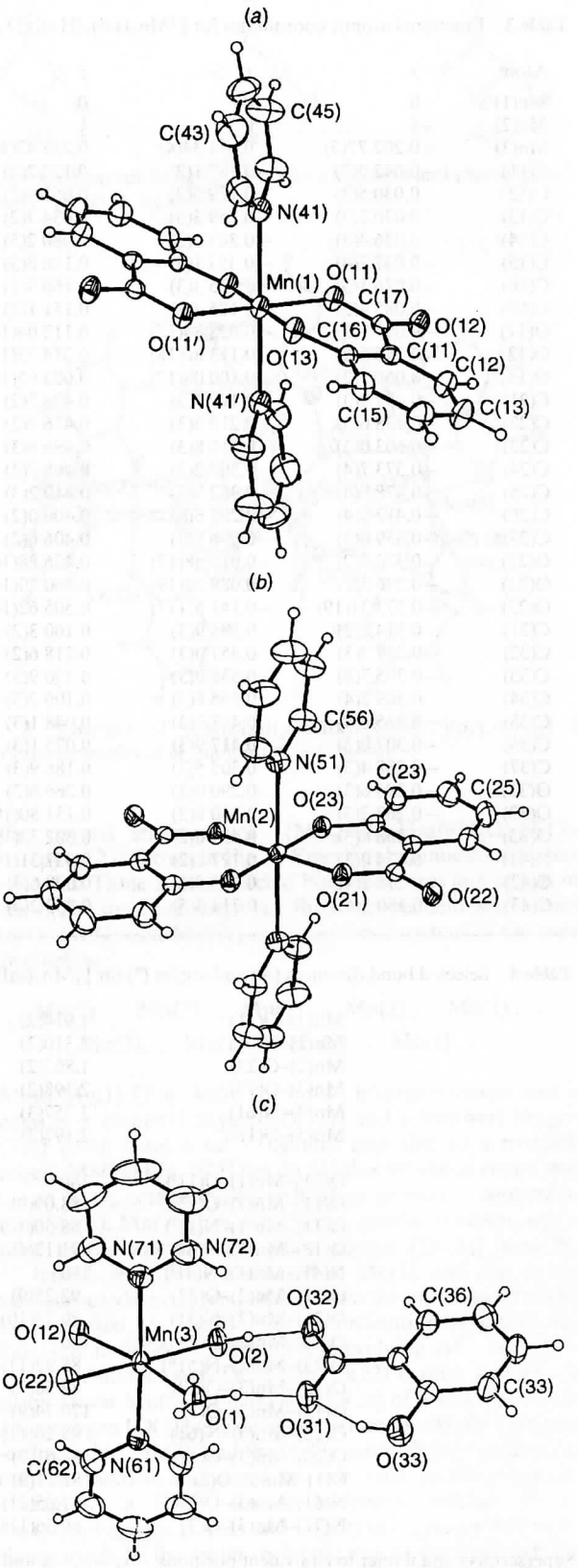

Fig. 4 Local co-ordination geometry around (*a*) Mn(1), (*b*) Mn(2) and (*c*) Mn(3) in complex **2**

Experimental

$[Mn_2(Hsal)_4(H_2O)_4]$ **1**.—To a solution of NaOH (0.436 g, 10.9 mmol) in water (150 cm^3) was added salicylic acid (1.513 g, 10.9 mmol) and $MnCl_2\cdot 4H_2O$ (1.039 g, 5.3 mmol). The resulting solution was refluxed for 3 h and then concentrated to *ca.* 50

cm^3). On standing for a few days at room temperature **1** formed as colourless crystals in 60% yield [Found (Calc.): C, 47.15 (46.05); H, 3.95 (3.85)%]. It is soluble in H_2O, EtOH, MeOH, dimethylformamide and tetrahydrofuran, and insoluble in diethyl ether. IR (KBr): $\tilde{\nu}/cm^{-1}$ (OH) 3700–2500, (CO_2) 1630, 1540, 1480, 1410. Λ_M (in H_2O) = 299 S cm^2 mol^{-1}.

$[Mn_2(sal)_2(Hsal)(H_2O)(H_3O)(py)_4{\cdot}2py\}_n]$ **2**. A dark green solution of **1** (1.0 g, 1.37 mmol) in pyridine (25 cm^3) was refluxed for 0.5 h. After cooling to room temperature dark green crystals of **2** slowly deposited over a period of a few days. The solid was filtered off, washed with diethyl ether and then air-dried. Yield 15% [Found (Calc.): C, 58.75 (59.40); H, 4.60 (4.70); N, 7.95 (8.15)%]. Complex **2** is soluble in EtOH, CH_2Cl_2, acetone, pyridine and dimethyl sulfoxide, and insoluble in diethyl ether. It dissolves in water to give a brown solution from which a brown solid quickly precipitates. Formation of this solid is accompanied by the smell of pyridine. IR (KBr): $\tilde{\nu}/cm^{-1}$ (OH) 3700–2100, (CO_2) 1620, 1560, 1535, 1440. UV/VIS (in EtOH): λ_{max} = 561 nm, ε = 276 dm^3 mol^{-1} cm^{-1}. Λ_M (in EtOH) = 5 S cm^2 mol^{-1}.

Hydrogen Peroxide Disproportionation Studies.—To a sample (*ca.* 10 mg) of the Mn salicylate complex was added aqueous H_2O_2 (35% w/w, 10 cm^3, 114 mmol). The mixture was stirred and thermostatted at 25 °C, and the O_2 evolved was measured volumetrically. In the cases where pyridine (1 cm^3) was added this was introduced into the reaction vessel before the addition of H_2O_2.

X-Ray Crystallography.—$[Mn_2(Hsal)_4(H_2O)_4]$ **1**. *Crystal data*. $C_{28}H_{28}Mn_2O_{16}$, M_r = 730.392, monoclinic, space group $P2_1/a$ (a non-standard orientation of no. 14), a = 7.626(1), b = 12.3150(9), c = 15.608(3) Å, β = 96.600(10)°, U = 1456.1(4) $Å^3$, Z = 2, D_c = 1.66 g cm^{-3}, $F(000)$ = 748, λ = 0.710 69 Å, μ(Mo-Kα) = 3.65 cm^{-1}.

A colourless crystal of approximate dimensions 0.3 × 0.3 × 0.3 mm was mounted on an Enraf-Nonius CAD4 diffractometer, and the intensities of 2436 reflections in the range $1 \leqslant \theta \leqslant 24°$ were measured using the ω–2θ scan mode and graphite-monochromated Mo-Kα radiation. Of 2231 unique reflections (R_{merg} = 0.0239) 1923 had $|F_{obs}| > 4\sigma|F_{obs}|$. Two reflections with χ between 80 and 90°, in the range $1 \leqslant \theta \leqslant 20°$, were chosen and measured to see if there was an absorption problem (h,k,l: 1,5,4/2,10,5). The data without the absorption factor were used to solve and refine the structure. The structure was solved using the direct method of SHELXS 86 followed, using SHELX 76,[14] by Fourier difference synthesis and refinement by full-matrix least squares to a conventional R factor of 0.0443. All the non-hydrogen atoms were refined anisotropically. The hydrogen atoms were located and refined individually with isotropic thermal parameters. The final stage of the refinement was to apply a weighting scheme to the data. This [$w = 1/\sigma^2(F_o)$] was refined to give a flat analysis of variance and R' of 0.0486. The goodness of fit was 2.0374 and the highest peak in the final electron-density map was found to be 0.53 e $Å^{-3}$.

$[\{Mn_2(sal)_2(Hsal)(H_2O)(H_3O)(py)_4{\cdot}2py\}_n]$ **2**. *Crystal data*. $C_{51}H_{48}Mn_2N_6O_{11}$, M_r = 1030.85, triclinic, space group $P\bar{1}$, a = 12.2736(13), b = 14.0642(12), c = 15.6015(18) Å, α = 94.134(18), β = 92.172(16), γ = 112.018(10)°, U = 2484.0(4) $Å^3$, Z = 2, D_c = 1.380 Mg m^{-3} $F(000)$ = 1069, λ = 0.710 69 Å, μ = 0.55 mm^{-1}, $2\theta_{max}$ = 50°.

A dark green crystal of dimensions 0.21 × 0.39 × 0.42 mm was mounted on a Nonius diffractometer, using the $\theta/2\theta$ scan mode. Cell dimensions were obtained from 25 reflections with 2θ angles in the range 19.00–32.00°. The h,k,l ranges used during structure solution and refinement were: $h_{min,max}$ −14, 14; $k_{min,max}$ = 0, 16; $l_{min,max}$ −18, 18. No. of reflections measured = 8697. No. of unique reflections = 8697. 5286 Reflections $I > 3.0\sigma(I)$. Absorption corrections were made. The minimum and maximum transmission factors were 0.800 and 0.867. The last least-squares cycle was calculated with 118 atoms, 635 parameters and 5286 out of 8697 reflections. Weights based on counting-statistics were used. The weighting scheme was $w = 1/[\sigma^2(F_o) + 0.0008F_o^2]$. The residuals were as follows: for significant reflections, R_F = 0.0378, R' = 0.0485, goodness of fit = 1.14; for all reflections, R_F = 0.0730, R' = 0.0602; $R_F = \Sigma(|F_o - F_c|)/\Sigma(F_o)$, $R' = \sqrt{[\Sigma w(F_o - F_c)^2/\Sigma(wF_o^2)]}$, and goodness of fit = $\sqrt{[\Sigma w(F_o - F_c)^2/(\text{no. of reflections} - \text{no. of parameters})]}$. The maximum shift/sigma ratio = 0.003. In the last electron-density map the deeepest hole was −0.230 e $Å^{-3}$, and the highest peak 0.230 e $Å^{-3}$. Secondary extinction coefficient = 0.187, and σ = 0.074. Program used and scattering factor data are given in refs. 15 and 16.

Additional material available from the Cambridge Crystallographic Data Centre comprises H-atom coordinates, thermal parameters and remaining bond lengths and angles.

Physical Measurements.—The IR spectra were recorded in the region 4000–200 cm^{-1} on a Perkin-Elmer 783 grating spectrometer and UV/VIS spectra were obtained using a Milton Roy Spectronic 3000 Array spectrometer. Magnetic susceptibility measurements were made using a Faraday balance and a Johnson Matthey magnetic susceptibility balance. Conductivity readings were obtained using an AGB Scientific model 10 conductivity meter. Cyclic voltammograms were recorded (*ca.* 20 °C and under dinitrogen) using an EG&G model 264A polarographic analyser and the data were analysed using the EG&G Condecon software package. A glassy carbon disc and a Pt wire were employed as the working and counter electrodes, respectively. Against a Ag–AgCl reference electrode the aqueous $[Fe(CN)_6]^{3-}$–$[Fe(CN)_6]^{4-}$ couple had $E_{\frac{1}{2}}$ = +0.29 V, and in ethanol the ferrocene–ferrocenium couple had $E_{\frac{1}{2}}$ = +0.58 V. Sample concentration was 4 × 10^{-3} mol dm^{-3}, and supporting electrolytes (0.1 mol dm^{-3}) in the aqueous and ethanol solutions were KCl and tetrabutylammonium perchlorate, respectively. Microanalytical data for the complexes were obtained by the Microanalytical Laboratory, University College Cork, Ireland.

Acknowledgements

We thank Dr. Charlie Harding (Open University, Milton Keynes) for variable-temperature magnetic susceptibility measurements. M. D. thanks Noel O'Reilly (Dublin Institute of Technology, DIT) for technical assistance, and M. Curran acknowledges the SRD funding scheme (DIT) for financial assistance.

References

1 M. Osawa, U. P. Singh, M. Tanaka, Y. Moro-oka and N. Kitajima, *J. Chem. Soc., Chem. Commun.*, 1993, 310 and refs. therein.
2 E. Bouwman, M. A. Bolcar, E. Libby, J. C. Huffman, K. Folting and G. Christou, *Inorg. Chem.*, 1992, **31**, 5185 and refs. therein.
3 J. B. Vincent, K. Folting, J. C. Huffman and G. Christou, *Inorg. Chem.*, 1986, **25**, 996.
4 C. Christmas, J. B. Vincent, H-R. Chang, J. C. Huffman, G. Christou and D. N. Hendrickson, *J. Am. Chem. Soc.*, 1988, **110**, 823.
5 W. Flaig, H. Beutelspacher and E. Rietz, *Soil Components*, ed. J. E. Gieseking, Springer-Verlag, New York, 1975, vol. 1, p. 1.
6 R. L. Rardin, W. B. Tolman and S. J. Lippard, *New J. Chem.*, 1991, **15**, 417; R. L. Rardin, A. Bino, P. Poganiuch, W. B. Tolman, S. Liu and S. J. Lippard, *Angew. Chem., Int. Ed. Engl.*, 1990, **29**, 812.
7 Y. Shi-Bao, S. J. Lippard, I. Shweky and A. Bino, *Inorg. Chem.*, 1992, **31**, 3502; A. Caneschi, F. Ferraro, D. Gatteschi, M. C. Melandri, P. Rey and R. Sessoli, *Angew. Chem., Int. Ed. Engl.*, 1989, **28**, 1365; K. Wieghardt, U. Bossek, B. Nuber, J. Weiss, J. Bonvoisin, M. Corbella, S. E. Vitos and J. J. Girerd, *J. Am. Chem. Soc.*, 1988, **110**, 7398; L. Que, jun. and A. E. True, *Prog. Inorg. Chem.*, 1990, **38**, 97.
8 F. A. Cotton and G. K. Wilkinson, *Advanced Inorganic Chemistry*, 5th edn., Wiley, New York, 1988, p. 702.
9 M. T. Casey, M. McCann, M. Devereux, M. Curran, C. Cardin, M. Convery, V. Quillet and C. Harding, *J. Chem. Soc., Chem. Commun.*, 1994, 2643.

10 E. J. Larson and V. L. Pecoraro, *Manganese Redox Enzymes*, ed. V. L. Pecoraro, VCH, New York, 1992, ch. 1 and refs. therein.
11 Y. Naruta and K. Maruyama, *J. Am. Chem. Soc.*, 1991, **113**, 3595.
12 P. N. Balasubramanian, E. S. Schmidt and T. C. Bruice, *J. Am. Chem. Soc.*, 1987, **109**, 7865.
13 E. J. Larson and V. L. Pecoraro, *J. Am. Chem. Soc.*, 1991, **113**, 3810.
14 G. M. Sheldrick, SHELX 76, University of Cambridge, 1976; SHELXS 86, University of Göttingen, 1986.
15 E. J. Gabe, Y. Le Page, J. P. Charland, F. L. Lee and P. S. White, *J. Appl. Crystallogr.*, 1989, **22**, 384.
16 *International Tables for X-Ray Crystallography*, Kynoch Press, Birmingham, 1974, vol. 4.

Received 27*th September* 1994; *Paper* 4/05910G